

A high-fidelity photon gun: intensity-squeezed light from a single molecule

Xiao-Liu Chu, Stephan Götzinger, and Vahid Sandoghdar

Max Planck Institute for the Science of Light, 91058 Erlangen, Germany

Department of Physics, Friedrich Alexander University, 91058 Erlangen, Germany

Graduate School in Advanced Optical Technologies (SAOT), 91058 Erlangen, Germany

August 30, 2016

A two-level atom cannot emit more than one photon at a time. As early as the 1980s, this quantum feature was identified as a gateway to “single-photon sources”, where a regular excitation sequence would create a stream of light particles with photon number fluctuations below the shot noise [1]. Such an intensity squeezed beam of light would be desirable for a range of applications such as quantum imaging, sensing, enhanced precision measurements and information processing [2, 3]. However, experimental realizations of these sources have been hindered by large losses caused by low photon collection efficiencies and photophysical shortcomings. By using a planar metallo-dielectric antenna applied to an organic molecule, we demonstrate the most regular stream of single photons reported to date. Measured intensity fluctuations reveal 2.2 dB squeezing limited by our detection efficiency, equivalent to 6.2 dB intensity squeezing right after the antenna.

Single-photon sources (SPS) have attracted a great deal of attention in the past two decades. One of the common methods for generating single photons is based on parametric down conversion in nonlinear materials, whereby a pair of photons are produced and separated using spectral, spatial, or polarization filters. Advantages of this approach are its large wavelength tunability and the possibility to herald the detection of one photon by the other one of the pair. However, the emission statistics in this method remains Poissonian, and it cannot produce single photons on demand.

To exclude the generation of two simultaneous photons, and more importantly, to achieve deterministic production of single photons at a given time, the antibunched radiation of an isolated quantum emitter offers the best choice [4–6]. However, so far random losses in the emission, collection, and detection processes have made it impossible to register one single photon at a particular time [7], so that the common terminologies of “single-photon” source or photon “gun” used in the literature greatly fall short of their expectations.

Three sources of loss have to be controlled. First, photophysical losses caused by a non-unity quantum efficiency (e.g. for color centers [8]) or unforeseeable transitions to dark states (e.g. in colloidal quantum dots [9]) spoil a deterministic emission. Second, it is a great challenge to collect all the photons, which are usually emitted in a nearly isotropic fashion. Third, the quantum efficiency of the detectors and losses in the optical path limit the final performance. Here, we present a substantial progress in remedying these issues by using single organic molecules with very high quantum efficiency as emitter, optimizing the excitation pulse scheme, careful choice of the optical elements, and employing a new design of metallo-dielectric antennas [10, 11].

The structure of the new antenna is depicted in Fig. 1a. By taking a standard cover glass as the high index bottom layer, we are able to use a microscope objective that works with a highly transmissive immersion oil. In the particular realization of our current work, we place a 30 nm thick PVA film (refractive index 1.5) on top of a 200 nm thick CYTOP layer (refractive index 1.35) to form a quasi-waveguide and subsequently spin coat a 20 nm layer of p-terphenyl, which is doped with terrylene molecules. These molecules are well known for their photostability at room temperature and fluoresce at a wavelength of about 590 nm [12]. As the top metallic mirror we used a gold-coated microprism, which we placed on top of polystyrene beads (diameter 1 μm) [13] to avoid the coupling of terrylene fluorescence to surface plasmons and consequent losses [10]. Using a combination of a planar antenna structure and an objective with a numerical aperture (NA) of 1.46, we can collect more than 99% of the emitted photons (see fig. 1b). The inset in Figure 1b shows the modified radiation pattern of a single oriented dipole inside the metallo-dielectric antenna.

The crystalline p-terphenyl sample is prepared at a low enough terrylene concentration such that these molecules are spatially well separated. Thus, as shown in Fig. 2a, each terrylene molecule can be individually addressed via p-polarized excitation in total internal reflection mode, appearing as a doughnut-shaped spot since its dipole orientation is nearly perpendicular to the interface [12]. The second-order correlation function shown in Fig 2b shows a value of $g^{(2)}(0) = 0.15$ and confirms the isolation of a single molecule. The measurement also indicates that a second photon might accompany the photon emitted by the molecule in about 7.5% of the excitations, consistent with the background fluorescence recorded on the sample next to the molecule. Considering that this background fluorescence can be modeled as a weak Poissonian light source, we can assume that the probability of simultaneous emission of two background photons is 0.3%. Since our detector is not number resolving, we measure the background at a given excitation power and account for it in the noise analysis.

The simplified energy level scheme of terrylene is shown in the inset of Fig. 2c. Considering an expected dark period of about 170 μs for the triplet state [14], we chose the excitation repetition rate to be as low as 15 kHz so that the interval between consecutive pulses is long enough for the molecule to return to the ground state before the arrival of the next excitation pulse. In this fashion, we reduced losses due to intersystem crossing to about 0.01%. Figure 2c shows the fluorescence signal of a single molecule as a function of the excitation power. The data is fitted with the function [15],

$$R(E_p) = R_0\rho(E_p) + \alpha E_p, \quad (1)$$

where E_p represents the pulse energy, $\rho(E_p)$ is the excited state population right after the excitation pulse, αE_p accounts for the background fluorescence, and R_0 is the maximum attainable photon count rate. Furthermore, the excited state population is given by [15]:

$$\rho(E_p) = \frac{E_p/E_s}{1 + E_p/E_s} (1 - e^{-(\tau_p/\tau_r)[1+(E_p/E_s)]}), \quad (2)$$

where E_s is the saturation energy, τ_p is the excitation pulse length, and τ_r is the lifetime of the excited state. It turns out that we can excite a molecule with 99% probability at about 200 pJ, which was the largest available pulse energy in our setup (Fig. 2c).

In addition to dark states, the quantum efficiency of the emitter can severely compromise the performance of a SPS. Figure 2d plots a histogram of the emission count rate for nearly 200 molecules upon strong excitation. While the quantum efficiency of terrylene in p-terphenyl is known to reach values beyond 95% [16], our measurements reveal a substantial inhomogeneity that leads to a distribution of the emitted powers. This behavior is also common for other solid-state systems such as color centers in diamond [8]. Thus, to achieve the lowest loss level, we performed our experiments on molecules with a high emission rate. In particular, the saturation measurement displayed in Fig. 2c was obtained on a molecule at an average count rate of 11400 counts/s, which is in very good agreement with the measured overall detection efficiency of 68%, excitation rate of 15 kHz, and a background level measured at 1100 counts/s (see Methods). In other words, we detect a photon on demand with a fidelity of about 70%.

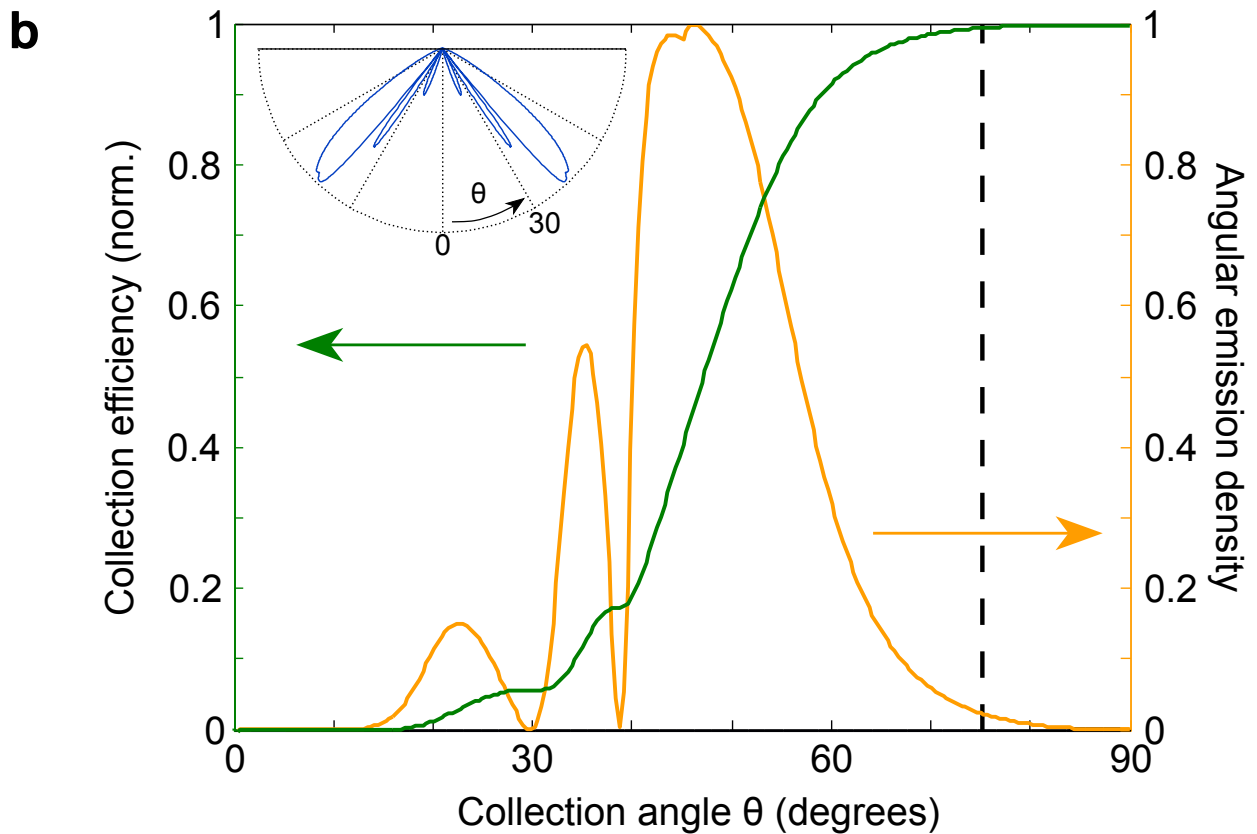
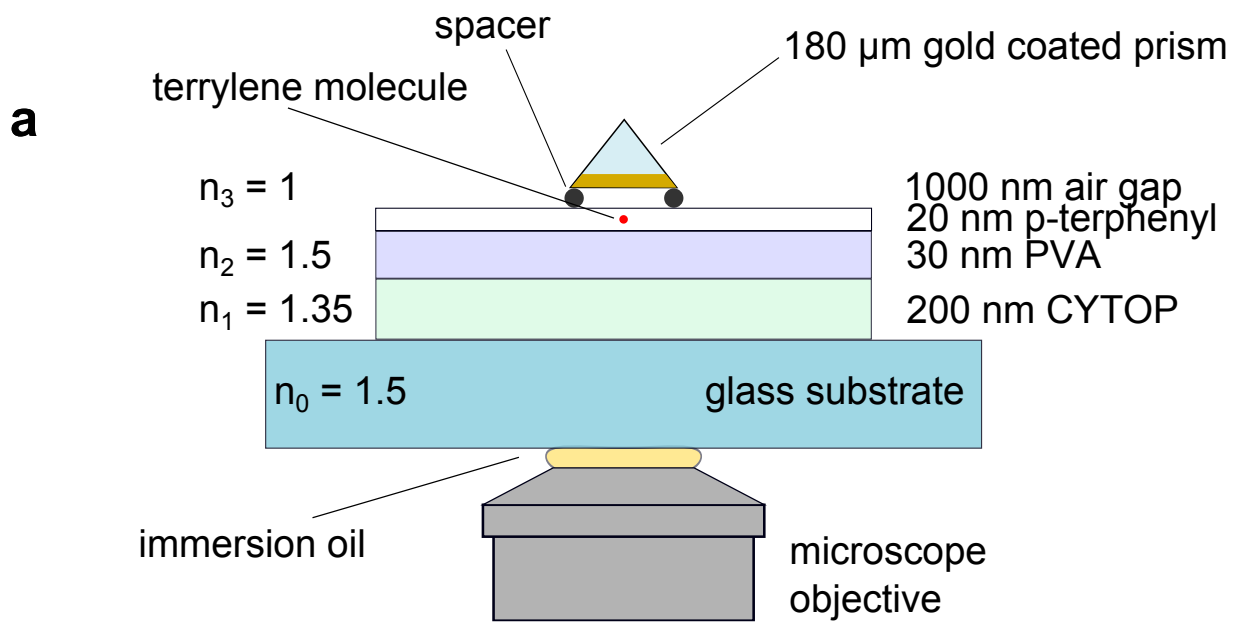


Figure 1: **Antenna design for 99% collection efficiency from a single molecule.** a, Sketch of the metallo-dielectric antenna. PVA and CYTOP act as quasi-waveguide on top of a cover glass, while a 180 μm gold coated prism prevents losses to the upper half space. Various elements are not drawn to scale. b, Emitted power density and collection efficiency as a function of the collection angle. The vertical dashed line indicates the maximum collection angle of the microscope objective. Inset: emitted power density in polar coordinates.

To portray the remarkable quality of our SPS, in the upper part of Fig. 3a we present a portion of the individual photon detection events over a period of 40 ms. A simple visual inspection confirms

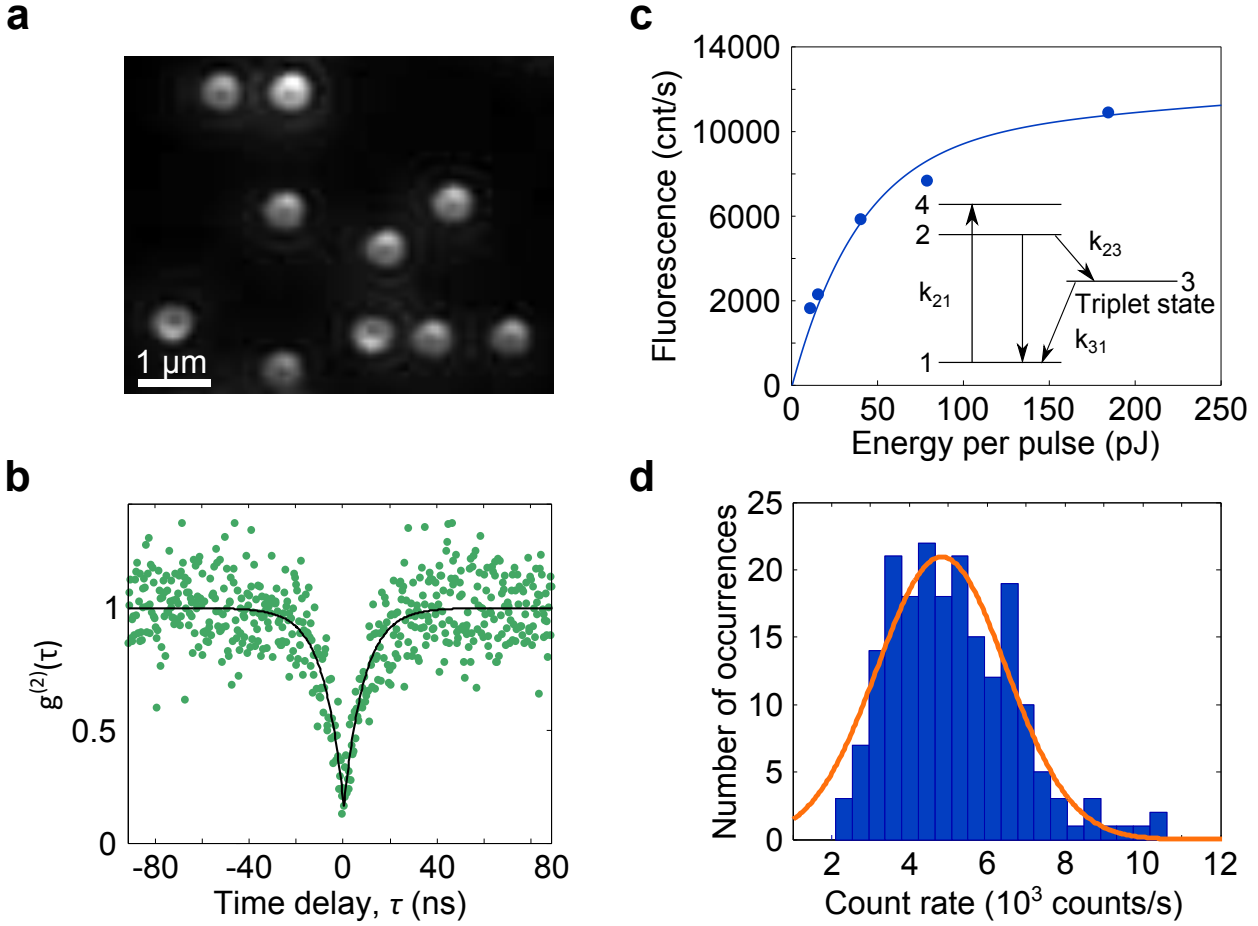


Figure 2: **Characterization of single-molecule single-photon sources.** a, Wide-field image of single molecules in the metallo-dielectric antenna. Individual terrylene molecules are clearly recognized by their characteristic doughnut pattern. b, Measured normalized second-order correlation function of a single molecules under continuous-wave strong excitation. c, Saturation measurement of a single molecule. The repetition rate of the pulsed laser was set to 15 kHz. Note the high photon detection rate due to the metallo-dielectric antenna. The inset shows a simplified Jablonski diagram with the relevant transition rates. $k_{21} \approx 1 \times 10^8$, $k_{23} \approx 1 \times 10^4$, $k_{31} \approx 6 \times 10^3$. d, Histogram of the fluorescence count rates obtained from 198 molecules driven at maximum pulse energy.

the high regularity of the photon arrivals. For comparison, in the lower part of the figure we emulate an example of a more typical SPS trace by lowering the excitation probability to 31% and, thus, lower efficiency.

For a quantitative demonstration of the SPS performance, we determine its sub-Poissonian nature from the actual detected count rate and its fluctuations (σ_{sps}). Figure 3b illustrates a time trace of the detected power. The blue distribution on the right panel shows that the intensity noise is reduced by 40% compared to the fluctuations (σ_{sn}) of a shot-noise limited source of the same intensity depicted in grey.

In Fig. 3c, we show $\sigma_{\text{sps}}/\sigma_{\text{sn}}$ for the same molecule as a function of the excitation pulse energy. The black theoretical curve takes into account the additional noise due to the background and provides a very good fit. In Fig. 3d, we display similar data for five different molecules plotted against the excited state population. Again, the data can be fitted very well.

The best result of our measurements reaches $\sigma_{\text{sps}}/\sigma_{\text{sn}} = 0.6$, corresponding to an intensity squeezing of 2.2 dB. The theoretically predicted ratio reads [2, 17]

$$\sigma_{\text{sps}}/\sigma_{\text{sn}} = \sqrt{1 - \zeta\rho}, \quad (3)$$

yielding a value of 0.62 ± 0.03 , in very good agreement with the experimental result, including

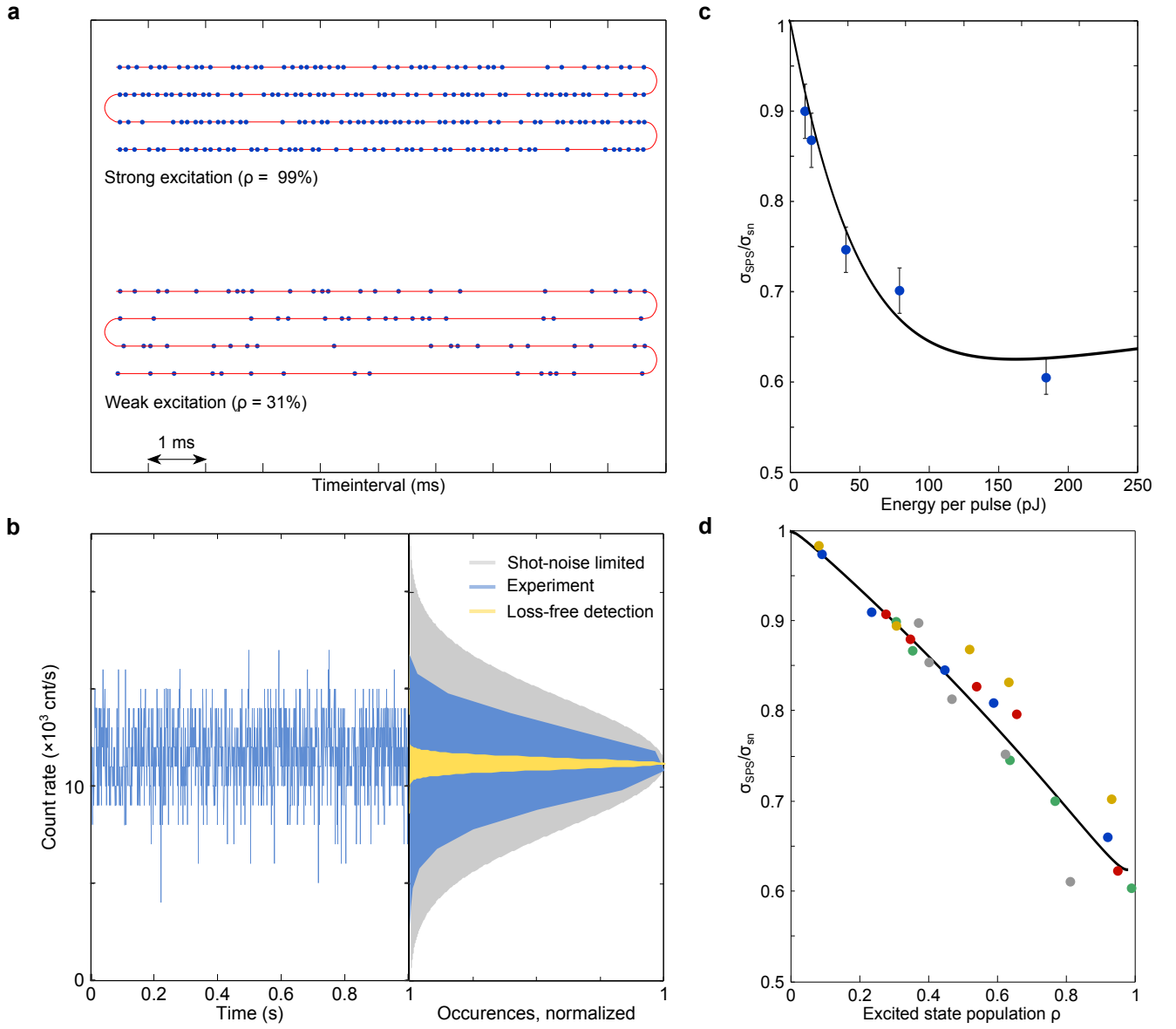


Figure 3: **A regular stream of single photons leads to intensity squeezed light.** a, Detection of single photons emitted by a molecular SPS. At high excitation energies ($\rho = 0.99$) the detection events are mostly regular whereas for the same molecule driven in the weak excitation regime ($\rho = 0.31$) the events become random. b, Left panel: Intensity trace of a strongly driven single molecule. Right panel: The measured intensity noise over 10 s (blue) is reduced by 40% compared to a shot-noise limited source of the same intensity. The yellow curve shows the noise distribution of the bare single-photon source including the contribution of background fluorescence, i.e. right after the antenna. c, Normalized intensity noise of a single-molecule single-photon source vs the excitation pulse energy. The positive slope of the theory curve at higher pulse energies originates from linearly increasing background. d, Measured intensity squeezing obtained from five different molecules (each shown in different color) and for various excited state populations $\rho(E_p)$ deduced from saturation measurements.

the measured background. Here, ζ denotes an overall detection efficiency, taking into account the photophysics of the emitter as well as losses in the detection path. The yellow curve presents the intrinsic noise distribution of our SPS once we eliminate the detection losses, which are currently dominated by the efficiency of our single-photon detector at a value of 80% (see Methods). This would yield $\sigma_{\text{SPS}}/\sigma_{\text{sn}} = 0.24$ equivalent to 6.2 dB intensity squeezing, limited by the background level of our sample.

A convenient measure for quantifying the sub-Poissonian nature of a SPS is the so-called Mandel

parameter given by $Q_D = [g^{(2)}(0) - 1]M\zeta\rho$, where M is the average number of photons per excitation pulse [18]. For an ideal SPS with unity detection efficiency, $Q_D = -1$, but Q_D is limited by the total efficiency ζ in any realistic experiment. The Mandel parameter for the overall detection efficiency of our experiment is -0.64 while the Q_D associated with our planar antenna amounts to -0.93. To our knowledge, these amount to the lowest Mandel parameters reported to date for a SPS.

Today, we are still faced with several challenges before SPSs can become available in a manner similar to lasers, i.e. at different wavelengths, bandwidths, or output power levels. To address some of these issues, various materials have been explored, including atoms [19, 20], molecules [18, 21, 22], quantum dots [23, 24], color centers [25], ions in traps [26, 27] and ions in a solid [28, 29]. In addition, different strategies for efficient collection of single photons have also been pursued, encompassing cavity-based concepts [30, 31] as well as wave guiding platforms [32–34]. The previous efforts do not reach a very high total efficiency and often require sophisticated fabrication or cryogenic operation. In this work, we have presented a straightforward and facile strategy for the generation of a photon on demand and have demonstrated its *detection* at a high fidelity of about 70%. This performance already surpasses the threshold reported for successful implementation of linear optical quantum computing [35], but foreseeable progress in detector technology should make it possible to still improve it by a considerable amount.

The sub-shot-noise light beam generated by a single quantum emitter is also very promising as a new intensity standard and can be used to calibrate photodetectors and counters at low light levels. By employing a low-loss mode conversion [36], we plan to couple our device to single mode fibers, delivering convenient sources of nonclassical light for various applications such as quantum key distribution [7, 37, 38], ultra-sensitive detection, imaging, and spectroscopy [39]. Our approach based on planar antennas is also applicable to other solid-state quantum emitters with high quantum efficiency.

Acknowledgements We thank Xue-Wen Chen for help with the antenna design and simulation. This project was supported by the European Union (ERC Advanced Grant SINGLEION and the SIQUTE project of the European Metrology Research Program (EMRP)), an Alexander von Humboldt professorship, and the Max Planck Society.

References

- [1] Mandel, L. Sub-poissonian photon statistics in resonance fluorescence. *Opt. Lett.* **4**, 205–207 (1979).
- [2] Lounis, B. and Orrit, M. Single-photon sources. *Rep. Prog. Phys.* **68**, 1129 (2005).
- [3] Polyakov, S. V. and Migdall, A. L. Quantum radiometry. *J. Mod. Opt.* **56**, 1045–1052 (2009).
- [4] Kimble, H. J., Dagenais, M., and Mandel, L. Photon antibunching in resonance fluorescence. *Phys. Rev. Lett.* **39**, 691–694 (1977).
- [5] Teich, M. C. and Saleh, B. E. A. Photon bunching and antibunching. *Prog. Optics* **26**, 1–104 (1988).
- [6] Kwiat, P. G. and Mattle, K. and Weinfurter, H. and Zeilinger, A. New high-intensity source of polarization-entangled photon pairs. *Phys. Rev. Lett.* **75**, 4337–4342 (1995).
- [7] Gisin, N., Ribordy, G., Tittel, W., and Zbinden, H. Quantum cryptography. *Rev. Mod. Phys.* **74**, 145–195 (2002).
- [8] Mohtashami, A. and Koenderink, A. F. Suitability of nanodiamond nitrogen-vacancy centers for spontaneous emission control experiments. *New J. Phys.* **15**, 043017 (2013).
- [9] Kuno, M., Fromm, D. P., Hamann, H. F., Gallagher, A., and Nesbitt, D. J. “on”/“off” fluorescence intermittency of single semiconductor quantum dots. *New J. Phys.* **115**, 1028 (2001).

- [10] Chen, X.-W., Göttinger, S., and Sandoghdar, V. 99% efficiency in collecting photons from a single emitter. *Opt. Lett.* **36**, 3545 (2011).
- [11] Chu, X.-L., Brenner, T. J. K., Chen, X.-W., Ghosh, Y., Hollingsworth, J. A., Sandoghdar, V., and Göttinger, S. Experimental realization of an optical antenna designed for collecting 99% of photons from a quantum emitter. *Optica* **1**, 203 (2014).
- [12] Pfab, R. J., Zimmermann, J., Hettich, C., Gerhardt, I., Renn, A., and Sandoghdar, V. Aligned terrylene molecules in a spin-coated ultrathin crystalline film of p-terphenyl. *Chem. Phys. Lett.* **387**, 490–495 (2004).
- [13] In some cases a slight roughness of the p-terphenyl film was sufficient as a spacer.
- [14] Lee, K., Chen, X.-W., Eghlidi, H., Kukura, P., Lettow, R., Renn, A., Sandoghdar, V., and Göttinger, S. A planar dielectric antenna for directional single-photon emission and near-unity collection efficiency. *Nature Photon.* **5**(3), 166–169 (2011).
- [15] Treussart, F., Alléaume, R., Floc’h, V. L., Xiao, L., Courty, J.-M., and Roch, J. Direct measurement of the photon statistics of a triggered single photon source. *Phys. Rev. Lett.* **89**, 1–4 (2002).
- [16] Buchler, B. C., Kalkbrenner, T., Hettich, C., and Sandoghdar, V. Measuring the quantum efficiency of the optical emission of single radiating dipoles using a scanning mirror. *Phys. Rev. Lett.* **95**, 063003 (2005).
- [17] Fox, M. *Quantum Optics: an introduction*. Oxford Univ. Press, New York, (2006).
- [18] Lounis, B. and Moerner, W. E. Single photons on demand from a single molecule at room temperature. *Nature* **407**, 491–493 (2000).
- [19] Kühn, A., Henrich, M., and Rempe, G. Deterministic single-photon source for distributed quantum networking. *Phys. Rev. Lett.* **89**(6), 067901, Jul (2002).
- [20] McKeever, J., Boca, A., Boozer, a. D., Miller, R., Buck, J. R., Kuzmich, A., and Kimble, H. J. Deterministic generation of single photons from one atom trapped in a cavity. *Science* **303**, 1992–1994 (2004).
- [21] Basché, T., Moerner, W. E., Orrit, M., and Talon, H. Photon antibunching in the fluorescence of a single dye molecule trapped in a solid. *Phys. Rev. Lett.* **69**(10), 1514–1517 (1992).
- [22] Lounis, B., Jelezko, F., and Orrit, M. Single molecules driven by strong resonant fields: Hyper-Raman and subharmonic resonances. *Phys. Rev. Lett.* **78**, 3673–3676 (1997).
- [23] Imamoglu, A. and Yamamoto, Y. Turnstile device for heralded single photons: Coulomb blockade of electron and hole tunneling in quantum confined p-i-n heterojunctions. *Phys. Rev. Lett.* **72**, 210–213 (1994).
- [24] Kim, J., Benson, O., Kan, H., and Yamamoto, Y. A single-photon turnstile device. *Phys. Rev. Lett.* **397**, 500–503 (1999).
- [25] Kurtsiefer, C., Mayer, S., Zarda, P., and Weinfurter, H. Stable solid-state source of single photons. *Phys. Rev. Lett.* **85**, 290–293 (2000).
- [26] Diedrich, F. and Walther, H. Nonclassical radiation of a single stored ion. *Phys. Rev. Lett.* **58**(3), 203–206, Jan (1987).

- [27] Keller, M., Lange, B., Hayasaka, K., Lange, W., and Walther, H. Continuous generation of single photons with controlled waveform in an ion-trap cavity system. *Nature* **431**(7012), 1075–1078 (2004).
- [28] Kolesov, R., Xia, K., Reuter, R., Stöhr, R., Zappe, A., Meijer, J., Hemmer, P. R., and Wrachtrup, J. Optical detection of a single rare-earth ion in a crystal. *Nature Comm.* **3**, 1029 (2012).
- [29] Eichhammer, E., Utikal, T., Göttinger, S., and Sandoghdar, V. High-resolution spectroscopy of single Pr^{3+} ions on the $^3\text{H}_4-^1\text{D}_2$ transition. *New J. Phys* **17**, 083018 (2015).
- [30] Strauf, S., Stoltz, N. G., Rakher, M. T., Coldren, L. A., Petroff, P. M., and Bouwmeester, D. High-frequency single-photon source with polarization control. *Nature Photon.* **1**, 704–708 (2007).
- [31] Michler, P., Kiraz, A., Becher, C., Schoenfeld, W. V., Petroff, P. M., Zhang, L., Hu, E., and Imamoglu, A. A quantum dot single-photon turnstile device. *Science* **290**, 2282–2285 (2000).
- [32] Liebermeister, L., Petersen, F., Münchow, A. V., Burchardt, D., Hermelbracht, J., Tashima, T., Schell, A. W., Benson, O., Meinhardt, T., Krueger, A., Stiebeiner, A., Rauschenbeutel, A., Weinfurter, H., and Weber, M. Tapered fiber coupling of single photons emitted by a deterministically positioned single nitrogen vacancy center. *Appl. Phys. Lett.* **104**, 1–3 (2014).
- [33] Claudon, J., Bleuse, J., Malik, N. S., Bazin, M., Jaffrennou, P., Gregersen, N., Sauvan, C., Lalanne, P., and Gerard, J.-M. A highly efficient single-photon source based on a quantum dot in a photonic nanowire. *Nature Photon.* **4**, 174–177 (2010).
- [34] Arcari, M., Söllner, I., Javadi, A., Lindskov Hansen, S., Mahmoodian, S., Liu, J., Thyrrestrup, H., Lee, E. H., Song, J. D., Stobbe, S., and Lodahl, P. Near-unity coupling efficiency of a quantum emitter to a photonic crystal waveguide. *Phys. Rev. Lett.* **113**, 1–5 (2014).
- [35] Varnava, M., Browne, D. E., and Rudolph, T. How good must single photon sources and detectors be for efficient linear optical quantum computation? *Phys. Rev. Lett.* **100**, 060502 (2008).
- [36] Labroille, G., Denolle, B., Jian, P., Genevieux, P., Treppe, N., and Morizur, J. F. Efficient and mode selective spatial mode multiplexer based on multi-plane light conversion. *Opt. Express* **22**, 518–519 (2014).
- [37] Scarani, V., Bechmann-Pasquinucci, H., Cerf, N. J., Dusek, M., Lütkenhaus, N., and Peev, M. The security of practical quantum key distribution. *Rev. Mod. Phys.* **81**, 1301–1350 (2009).
- [38] Waks, E., Santori, C., and Yamamoto, Y. Security aspects of quantum key distribution with sub-poisson light. *Phys. Rev. A* **66**, 042315 (2002).
- [39] Brida, G., Genovese, M., and Ruo Berchera, I. Experimental realization of sub-shot-noise quantum imaging. *Nature Photon.* **4**, 227–230 (2010).

Methods

Sample fabrication. Cover glasses (170 μm thickness) were cleaned in an oxygen plasma followed by treatments in methanol, ethanol and isopropanol to remove any organic contamination. Next, a 200 nm layer of CYTOP was spin coated onto the cleaned cover glass and a 4 nm layer of TiO_2 was deposited on top. A 30 nm layer of polyvinylalcohol (PVA) was then used to protect the CYTOP (AGC Chemicals europe ltd.). A solution of toluene containing terrylene and p-terphenyl molecules was then spin coated [12]. Finally, we placed a 180 μm gold coated prism onto the sample. However, to allow for sufficient space between the gold layer and the molecule (i.e., avoid coupling to surface plasmons), polystyrene beads were distributed on the p-terphenyl layer first. We confirmed a typical gap of 800-1000 nm by back focal plane imaging of single molecules.

Experimental setup. To excite the terrylene molecules, we used a pulsed laser (time-bandwidth Cheetah-X-SHG) with a pulse width of 13 ps at a wavelength of 532 nm. After the laser we inserted a pulse picker in order to reduce the repetition rate of the laser to 15 kHz. The light was focused to an area of about $1\ \mu\text{m} \times 1\ \mu\text{m}$ via total internal reflection through the microscope objective. By setting the incident light to be p-polarized, we ensured efficient excitation of the vertically oriented molecular dipole moments. Photons emitted by the molecules were collected by the same microscope objective, separated from the excitation light by a long-pass filter (Semrock, 538 nm) and detected by a sensitive CCD camera, a single-photon counter or a Hanbury-Brown and Twiss photon correlator.

In order to minimize losses, we optimized the setup for a high photon detection efficiency. The photons were collected by an immersion objective (Zeiss alpha Plan-Apochromat 100x/1.46, collection angle 74° degrees) with a transmission of $90 \pm 2\%$. The losses of all the optical components, including mirrors, lenses and filters added up to $5 \pm 2\%$. The single photon detector (Laser 2000) had a quantum efficiency of $80 \pm 4\%$ at 605 nm. This allows us to determine the total detection efficiency ζ to be as high as $68 \pm 3\%$.

Noise analysis. We model all losses including the detector inefficiency by a single beam splitter with splitting ratio $T/(1 - T)$, where the transmission T is equivalent to the total probability of detecting a photon upon excitation of the single molecule [17]. The beam splitter process occurs at the single photon level randomly with a weighted probability of T and $(1 - T)$, respectively, according to random sampling. The randomness induced by the beam splitter increases the noise in the transmitted single photon stream towards Poissonian statistics. In order to study the intensity fluctuations of our SPS, we record the photon flux over a period of 10 s and divide the obtained data into time bins of length 1 ms. By looking at the variation of the number of detected photons in the time bins, we obtain the intensity noise of the SPS. For the theoretical analysis we model our source as a single emitter where we detect the emitted photons with a certain total detection efficiency and an uncorrelated linear background. The standard deviation is therefore given by:

$$\sigma_{\text{sps}}(E_p) = \sqrt{\sigma_{\text{mol}}^2(E_p) + \sigma_{\text{bg}}^2(E_p)},$$

where σ_{mol} and σ_{bg} is the noise originating from variations in photons emitted by the single molecule and the Poissonian noise of the background, respectively. Note that the intensity noise of the emitter $\sigma_{\text{mol}}(E_p) = \sqrt{1 - \zeta\rho(E_p)} \sigma_{sn}$ contains all loss channels including the detector efficiency and excitation probability.